



## Abstract

We investigate the relationship between climate and tree-ring data on a global scale using the process-based Vaganov–Shashkin–Lite (VSL) forward model of tree-ring width formation. The VSL model requires as inputs only latitude, monthly mean temperature, and monthly accumulated precipitation. Hence, this simple, process-based model enables ring-width simulation at any location where monthly climate records exist. In this study, we analyse the growth response of simulated tree-rings to monthly climate conditions obtained from the CRU TS3.1 data set back to 1901. Our key aims are (a) to examine the relations between simulated and observed growth at 2287 globally distributed sites and (b) to evaluate the potential of the VSL model to reconstruct past climate. The assessment of the growth-onset threshold temperature of approximately 4–6 °C for most sites and species using a Bayesian estimation approach complements other studies on the lower temperature limits where plant growth may be sustained. Our results suggest that the VSL model skilfully simulates site level tree-ring series in response to climate forcing for a wide range of environmental conditions and species. Spatial aggregation of the tree-ring chronologies to reduce non-climatic noise at the site level yields notable improvements in the coherence between modelled and actual growth. The resulting distinct and coherent patterns of significant relationships between the aggregated and simulated series further demonstrate the VSL model's ability to skilfully capture the climatic signal contained in tree-series. Finally, we propose that the VSL model can be used as an observation operator in data assimilation approaches to reconstruct past climate.

## 1 Introduction

Information derived from tree-rings is one of the most powerful tools available for studying past climatic variability as well as identifying fundamental relationships between tree-growth and climate (e.g. Fritts, 1976; Briffa et al., 2002a, b; IPCC, 2007). Tree-ring

CPD

9, 4065–4098, 2013

## Forward modelling of tree-ring width

P. Breitenmoser et al.

[Title Page](#)

[Abstract](#)

[Introduction](#)

[Conclusions](#)

[References](#)

[Tables](#)

[Figures](#)

[◀](#)

[▶](#)

[◀](#)

[▶](#)

[Back](#)

[Close](#)

[Full Screen / Esc](#)

[Printer-friendly Version](#)

[Interactive Discussion](#)



---

**Forward modelling  
of tree-ring width**P. Breitenmoser et al.

---

[Title Page](#)[Abstract](#)[Introduction](#)[Conclusions](#)[References](#)[Tables](#)[Figures](#)[|◀](#)[▶|](#)[◀](#)[▶](#)[Back](#)[Close](#)[Full Screen / Esc](#)[Printer-friendly Version](#)[Interactive Discussion](#)

archives offer many advantages for climate reconstructions including their wide spatial distribution, annual resolution, calendar-exact dating, and high climate sensitivity (Hughes, 2002; Jones et al., 2009). However, relationships between tree-growth and climate are complex and classical calibration methods (i.e., establishing a statistical relationship between instrumental and proxy data during their period of overlap) are often inadequate for several reasons. Firstly, empirical methods generally treat climate as a function of the proxy rather than quantify how proxy signals are driven by climate variability. Secondly, statistical calibration is bound by assumptions of uniformitarianism and stationarity in the climate-growth system – conditions that may not be adequately met (Raible et al., 2006). Thirdly, most tree-ring based reconstructions are limited to geographic regions where growth variability is predominantly constrained by a single environmental variable. For example, temperature reconstructions are limited to regions where growth is primarily limited by cold temperatures – leaving the vast areas of the Earth away from high mountains and high latitude environments poorly represented by high-quality proxy data (Wahl and Frank, 2012).

In recent years, data assimilation approaches have found an increasingly important role in palaeoclimatic reconstruction efforts (Hughes and Ammann, 2009; Trouet et al., 2009; Goosse et al., 2010; Widmann et al., 2010; Franke et al., 2011; Bhend et al., 2012; Tingley et al., 2012). Combined information from climate models and proxy archives, including also associated errors and their covariance, provide a physically plausible representation of past climate consistent with available proxy data. An observation operator, which expresses the proxy as a function of the model data, is the formal link between model and proxy data. So-called forward proxy models (process-based or empirical) could potentially be used as an observation operator in data assimilation approaches (Hughes and Ammann, 2009).

The Vaganov–Shashkin (VS; Vaganov et al., 2006, 2011) process-based forward model has been demonstrated to skilfully simulate tree-ring width in North America and Siberia (Anchukaitis et al., 2006; Evans et al., 2006; Vaganov et al., 2011), China (Shi et al., 2008; Zhang et al., 2011), and Tunisia (Touchan et al., 2012). This forward-model

---

**Forward modelling  
of tree-ring width**P. Breitenmoser et al.

---

[Title Page](#)[Abstract](#)[Introduction](#)[Conclusions](#)[References](#)[Tables](#)[Figures](#)[I ◀](#)[▶ I](#)[◀](#)[▶](#)[Back](#)[Close](#)[Full Screen / Esc](#)[Printer-friendly Version](#)[Interactive Discussion](#)

of tree-ring growth was developed to establish non-linear and non-stationary relationships between climate variables and tree-ring formation (Vaganov et al., 2006, 2011), yet applications generating “pseudo ring-width” series from global climate models has so far been hindered by the relative complexity. Recently, Tolwinski-Ward et al. (2011a, b) introduced a simplified model version (the so-called Vaganov–Shashkin–Lite; VSL model) that skilfully reproduced climate-driven variability in North American tree-ring width chronologies. This simple and efficient model of non-linear climatic controls on tree-ring width requires only latitude, monthly temperature, and monthly precipitation as inputs and has the potential to simulate tree-rings across a wide range of environments, species, and spatial scales. The VSL model is hence a promising candidate for palaeoclimate reconstruction.

The goals of this study are to (i) examine the model's ability to skilfully link climate and tree-ring formation across the globe, (ii) identify large-scale patterns of the climatic drivers of tree growth, and (iii) evaluate the suitability of forward modelling of tree-rings in a reconstruction approach. This study is the first report examining the VSL model's application on a global scale, and thereby across a wide range of species and site conditions, using a gridded data set based on direct observations from meteorological stations. All suitable raw tree-ring width measurements from the International Tree Ring Database (ITRDB) are analysed in a comparable way. Results of such an intercomparison may help to make better use of tree-ring information in climate reconstructions.

The paper is organised as follows: we provide a brief introduction to the climate data, the structure and parameterisations of the VSL model, and the tree-ring chronologies. The main results and discussion detailing the coherence between observed and simulated growth and associated climatic controls across space and over time are then presented. Lastly, we provide conclusions and make suggestions for further analyses.

## 2 Data and methods

### 2.1 Climate data

The climate data used to simulate tree-ring growth are monthly CRU TS3.1 mean near surface temperature and CRU TS3.1.1 precipitation data sets from the Climatic Research Unit (CRU; Mitchell and Jones, 2005). These data cover the global land surface (except for Antarctica) at a  $0.5^\circ \times 0.5^\circ$  spatial resolution from 1901–2009 (updated from Mitchell and Jones, 2005; <http://badc.nerc.ac.uk/data/cru>) and are based on direct observations from meteorological stations. As the underlying data should be kept in mind when interpreting results, it is important to note that the temporal and spatial density of the underlying observations is variable and interpolation over greater distances is routinely performed (Jones et al., 1997). Comparison with the available network of tree-rings (see Fig. 1 for locations) shows, for instance, that both the instrumental and tree-ring networks are dense for the European Alps, but very sparse for many tropical regions such as the Amazon. On the other hand, tree-ring chronologies are much more prevalent in the boreal zone, such as in the vast areas of Siberia and northern Canada while instrumental data in India dominate over the available tree-ring network.

### 2.2 Forward model description: the VSL model

We use the Vaganov–Shashkin–Lite (VSL) model to produce synthetic tree-ring chronologies (Tolwinski-Ward et al., 2011a, b; version 2.2 accessible from <http://www.ncdc.noaa.gov/paleo/softlib/softlib.html>). This process-based forward model assumes that climatic influences can be associated directly, but non-linearly with tree-ring growth. The VSL model only requires monthly mean temperature, accumulated precipitation, and latitude to model growth. A further 12 adjustable parameters are required related to climatic limitations on growth, parameterizations for soil moisture availability, and the calendar periods when annual increment of wood is responsive to climate. In comparison, the full Vaganov–Shashkin model depends on daily climate input variables

CPD

9, 4065–4098, 2013

## Forward modelling of tree-ring width

P. Breitenmoser et al.

Title Page

Abstract

Introduction

Conclusions

References

Tables

Figures

◀

▶

◀

▶

Back

Close

Full Screen / Esc

Printer-friendly Version

Interactive Discussion



## Forward modelling of tree-ring width

P. Breitenmoser et al.

Title Page

Abstract

Introduction

Conclusions

References

Tables

Figures

◀

▶

◀

▶

Back

Close

Full Screen / Esc

Printer-friendly Version

Interactive Discussion



and has over 40 tunable parameters (Vaganov et al., 2006, 2011). Although detailed mechanistic processes such as photosynthesis, storage, or cambial cellular processes are not modelled directly in VSL, the net effect of the dominating nonlinear climatic controls on tree-growth are implemented in terms of the principle of limiting factors and threshold growth response functions. Despite its simplicity, simulations using VSL have been shown to skilfully reproduce climate-driven variability in North American tree-ring width chronologies (Tolwinski-Ward et al., 2011a, b).

For a specific site and given month  $i$ , growth is calculated from the minimum of the growth responses to temperature ( $g_T$ ) and moisture ( $g_M$ ), modulated by the response to insolation ( $g_E$ ):

$$G(i) = g_E(i) \cdot \min \{g_T(i), g_M(i)\}. \quad (1)$$

Annual ring width is then defined as the sum of the monthly growth increments  $G(i)$  over a specified growth period  $I$  (Tolwinski-Ward et al., 2011a):

$$\text{TRW}_{\text{VSL}} = \sum_{i \in I} G(i). \quad (2)$$

In Eq. (1),  $g_E$  is the ratio of mean monthly day length  $L$  relative to that in the summer solstice month at the corresponding latitude, computed using standard trigonometric approximations:

$$g_E(i) = \frac{L(i)}{\max\{L(i)\}} \quad (3)$$

The partial growth rates  $g_T$  and  $g_M$  are defined as ramp functions, with growth parameters representing climate thresholds below which temperature  $T$  and moisture  $M$  are not high enough for growth ( $T_1, M_1$ ), and thresholds above which temperature or moisture sustain non-limited growth ( $T_2, M_2$ ). Values of these partial growth responses are between zero and one (Tolwinski-Ward et al., 2011a):

$$g_T(i) = \begin{cases} 0 & \text{for } T(i) \leq T_1 \\ \frac{T(i)-T_1}{T_2-T_1} & \text{for } T_1 < T(i) \leq T_2 \\ 1 & \text{for } T(i) > T_2 \end{cases} \quad (4)$$

$$g_M(i) = \begin{cases} 0 & \text{for } M(i) \leq M_1 \\ \frac{M(i)-M_1}{M_2-M_1} & \text{for } M_1 < M(i) \leq M_2 \\ 1 & \text{for } M(i) > M_2 \end{cases} \quad (5)$$

A Bayesian estimation approach with a uniform prior distribution of the VSL growth response parameters is performed to find the optimal parameters  $T_1$ ,  $T_2$ ,  $M_1$ , and  $M_2$  for each site. In addition to the Bayesian parameter estimation approach, we also estimated optimal parameters for every site using a simple optimisation procedure as described in Tolwinski-Ward et al. (2011a). Parameters were sampled uniformly across intervals and the parameter set producing the simulation that correlated most significantly with the corresponding observed series was then used to simulate the tree-ring series (note that throughout this paper we use Pearson correlation coefficients). Results from both parameter estimation approaches are generally similar, with some evidence that the parameter optimisation approach sometimes result in model over-fitting due to the correlation constraint imposed. Nevertheless, the comparable results support the validity of either of these approaches with some possible advantages for the Bayesian parameter estimation (Tolwinski-Ward et al., 2011a, 2013).

Soil moisture  $M(i)$  is calculated from monthly temperature and accumulated precipitation data,  $T(i)$  and  $P(i)$ , via the empirical Leaky Bucket model of hydrology from the National Oceanic and Atmospheric Administration's Climate Prediction Center (CPS), allowing for sub-monthly updates of soil moisture to account for the non-linearity of the soil moisture response (Huang et al., 1996; Tolwinski-Ward et al., 2011a; codes available from <http://www.ncdc.noaa.gov/paleo/softlib/softlib.html>).

In addition to the four parameters controlling the simulated growth response to temperature and soil moisture, all other parameters are taken from published studies (e.g.,

**Forward modelling of tree-ring width**

P. Breitenmoser et al.

Title Page	
Abstract	Introduction
Conclusions	References
Tables	Figures
◀	▶
◀	▶
Back	Close
Full Screen / Esc	
Printer-friendly Version	
Interactive Discussion	



Huang et al., 1996; van den Dool et al., 2003; Fan and van den Dool, 2004; Evans et al., 2006; Vaganov et al., 2006; Tolwinski-Ward et al., 2011a; Zhang et al., 2011; Touchan et al., 2012), as is outlined in Table 1. Those studies have demonstrated the ability to apply the parameters to a wide range of environmental conditions. Thus, model generality is emphasized in the choice of parameters and modelling procedure.

As growth period  $I$  we chose a 16 month interval, starting in previous September and ending in December of the modelled year (previous March to current June for the Southern Hemisphere). This integration interval has been selected to (a) account for persistence in tree-ring growth (leading to autocorrelation), (b) showed best overall performance in a subset of regions, and (c) has been used successfully by Tolwinski-Ward et al. (2011a) in their simulations of North American tree-ring series.

The final  $TRW_{VSL}$  series were then standardized based on the 1901–1970 period.

### 2.3 Tree ring-chronologies

Raw tree-ring width measurements from 2918 sites from 163 different tree species were obtained from the International Tree Ring Database (ITRDB; Grissino-Mayer and Fritts, 1997; <http://www.ncdc.noaa.gov/paleo/treering.html>). Prior to further analysis, we attempted to identify and correct data and metadata errors including repetitive measurements, feet-meter encoding, inappropriate decimal points and hyphenations, incorrect series labelling, or misplaced series positions (see Table S1 in the Supplement).

To remove the biological age-trend and other lower-frequency signals that may be driven by stand dynamics or disturbances, we processed all data sets in the program ARSTAN (Cook, 1985) using standard dendroclimatological methods (i.e., detrending and transformation to dimensionless growth indices). We tested different standardising methods on a subset of 97 locations from all six continents to infer the most applicable detrending option to our data. Methods tested include (a) a negative exponential curve and linear regression fits, (b) a smoothing spline fit with a 50 % frequency response cut-off (which is the wavelength at which 50 % of the amplitude of a signal is retained) equal to 3/4 of a series length, and (c) a smoothing spline with a 200 yr frequency response

## Forward modelling of tree-ring width

P. Breitenmoser et al.

Title Page

Abstract

Introduction

Conclusions

References

Tables

Figures

◀

▶

◀

▶

Back

Close

Full Screen / Esc

Printer-friendly Version

Interactive Discussion



## Forward modelling of tree-ring width

P. Breitenmoser et al.

Title Page

Abstract

Introduction

Conclusions

References

Tables

Figures

◀

▶

◀

▶

Back

Close

Full Screen / Esc

Printer-friendly Version

Interactive Discussion



cut-off. These tests and Pearson correlation analyses between the differently standardised series and the monthly climate parameters favour a hierarchical approach: fitting negative exponential curves and linear regression curves of any slope were applied as first order detrending options but if these two methods were not suitable (e.g., because values of a fitted curve approached zero), a smoothing spline was fit with a 50 % cut-off frequency at 75 % of each series length. The detrending methods applied will allow retention of climate-related signals in any given chronology on the order of the median maximum segment length of the constituent tree-ring series (Cook et al., 1995).

Combining multiple measurements into a single ring-width chronology should then ideally represent a coherent climate signal of a particular species at a site (Cook et al., 1990). Standard chronologies ( $TRW_{ITRDB}$ ) of all these sites were developed by a bi-weight robust mean estimate (Cook et al., 1990) and the variance was stabilized to minimize artefacts from changing sample size through time (Osborn et al., 1997; Frank et al., 2007). Further, we required that the sample depth of a chronology (number of samples from trees used for every point in time) is always  $\geq 8$  and that the 1901–1970 interval is fully covered by tree-ring data. These criteria resulted in 2287 chronologies for further analyses

### 3 Results and discussion

#### 3.1 Quality indicators for tree-ring chronologies

Understanding of the specific characteristics of the tree network is essential to interpret the modelled tree-ring chronologies. Various chronology characteristics of all 2287 ring-width chronologies ( $TRW_{ITRDB}$ ) for the 1901–1970 common period were computed (Fig. 2; see Fig. 1 for locations). The average inter-series correlation between all series in a chronology ( $R_{bar}$ ) indicates common variance (Cook et al., 1990) while the expressed population signal (EPS) measures the similarity of a chronology to a hypothetical population chronology. The latter is used to determine over which time intervals

---

**Forward modelling  
of tree-ring width**P. Breitenmoser et al.

---

[Title Page](#)[Abstract](#)[Introduction](#)[Conclusions](#)[References](#)[Tables](#)[Figures](#)[I◀](#)[▶I](#)[◀](#)[▶](#)[Back](#)[Close](#)[Full Screen / Esc](#)[Printer-friendly Version](#)[Interactive Discussion](#)

5 a chronology can be regarded to meet the population chronology to some acceptable degree (Wigley et al., 1984). An EPS threshold value, following the example in Wigley et al. (1984), of 0.85 is routinely cited in dendrochronological literature. Running Rbar and EPS statistics were calculated over moving 30 yr windows with 15 yr overlap. 93 %  
10 of all mean EPS values in our network are above 0.85 over the 1901–1970 time period. Rbar values roughly follow a normal distribution with a mean of 0.39. These statistics suggest that the vast majority of chronologies have a relatively robust signal that should allow climatic drivers to be inferred. Typical tree-ring chronologies have a mean segment length of 170 yr and a sample depth of 30 series per chronology. However,  
15 these distributions have relatively long tails reflecting exceptionally well-replicated sites or sites with long-lived tree species (e.g., Bristlecone pine). The mean segment and our detrending approach suggest that we should be able to test inter-annual to (at least) multi-decadal variability in our modelling efforts. The geographical distribution of the sites is dominated by low-altitudes and the mid-latitudes, but there are also a considerable amount of high-latitude and high elevation sites particularly in the Northern Hemisphere.

### 3.2 Parameter estimation

20 Site specific growth parameters ( $T_1$ ,  $T_2$ ,  $M_1$ , and  $M_2$ ) are necessary due to diverse environmental conditions, site ecologies, and species represented in this global network. Accordingly, the VSL growth response function parameters were determined for each chronology via Bayesian parameter estimation using temperature, precipitation, site latitude, and ring-width data during the calibration interval. This scheme assumes uniform priors for the growth response parameters, and independent, normally distributed errors for the ring-width model. The median of each of the growth parameters in the  
25 resulting posterior probability distribution was finally taken as the “calibrated” growth response values for a particular site. A more detailed description of the approach can be found in Tolwinski-Ward et al. (2013).

## Forward modelling of tree-ring width

P. Breitenmoser et al.

Title Page

Abstract

Introduction

Conclusions

References

Tables

Figures

◀

▶

◀

▶

Back

Close

Full Screen / Esc

Printer-friendly Version

Interactive Discussion



For calibration/verification purposes, we divided the period 1901–1970 into two equal 35yr long intervals and alternately withhold the first or second half for verification. Descriptive statistics of the parameter estimation for the 1901–1935 and 1936–1970 calibration intervals are provided in Table 2. Even though the response parameters were calculated independently, the results are very consistent across the two intervals, showing skill in the growth response parameter estimation.

Figure 3 further illustrates the estimated temperature and moisture parameters  $T_1$ ,  $T_2$ ,  $M_1$ , and  $M_2$  for each site and different tree genera. The parameter estimation of the VSL model provides further insight into the currently debated (Mann et al., 2012; Anchukaitis et al., 2012) temperature threshold below which growth may no longer take place. We find a growth-onset threshold temperature ( $T_1$ ) of approximately 4–6°C for most sites and species with all estimates between 1.80°C and 8.41°C (see also Table 2). A similar threshold temperature range was found by Tolwinski-Ward et al. (2013) who used a four parameter beta distribution to calibrate the model parameters on a subset of 277 series in the United States. These findings compare favourably with assessments of growing season temperatures at treeline based upon in-situ loggers or remote sensing and interpolated climatic data (Körner and Paulsen, 2004; Körner, 2012), as well as observational studies of wood formation (Rossi et al., 2007).

Sites of tree-ring chronologies are, on average, located 164 m higher than the elevation of the corresponding CRU grid cell. Hence, we attempted to correct temperature for elevational differences between the CRU and the tree sites by considering a mean lapse rate of  $0.65\text{ °C (100 m)}^{-1}$  (Wallace and Hobbs, 2006), yet the average correlation between  $\text{TRW}_{\text{VSL}}$  and  $\text{TRW}_{\text{ITRDB}}$  slightly decreased. As we do not completely understand the causes for this insignificant drop, we do not correct for elevational differences. Hence, our estimates may slightly overestimate the threshold temperatures and represents a conservative estimate of conditions under which growth occurs.

We also examined whether the range of values obtained indeed reflect differential growth limitations as related to site conditions or tree species (Fig. 3). For instance, Vaganov et al. (2006), based on the VS-model, reported minimum and optimal

## Forward modelling of tree-ring width

P. Breitenmoser et al.

[Title Page](#)

[Abstract](#)

[Introduction](#)

[Conclusions](#)

[References](#)

[Tables](#)

[Figures](#)

[I ◀](#)

[▶ I](#)

[◀](#)

[▶](#)

[Back](#)

[Close](#)

[Full Screen / Esc](#)

[Printer-friendly Version](#)

[Interactive Discussion](#)



temperatures in the northern Taiga of 4 °C and 16 °C for larch, 6 °C and 18 °C for spruce, and 5 °C and 18 °C for Scots pine, respectively. We find comparable results using VSL (Fig. 3a–d). For spruce, our estimates of  $T_1$  and  $T_2$  are generally higher than for pine trees while  $M_2$  is lower. This might reflect the better adaptation of pines to lower temperature conditions and drought. We also find differences within the pine species. For Ponderosa and Pinyon pines,  $T_1$  is about 1 to 2 °C lower than for other pine species (Fig. 3e, compare also to Fig. 3a in which these two species clearly influence the shape of the pine histogram towards cooler threshold temperatures). These results contribute to understanding species-specific growth responses documented for a wide range of tree species (Babst et al., 2013).

As to what concerns the moisture parameters, species-related differences due to needle structure as well as frequency and density of stomata might influence water loss due to evapotranspiration (Vaganov et al., 2006). However, uncertainties arise from the parametrisation of  $M$  and estimation of  $M_1$  and from the missing representation of winter precipitation stored as snow pack in the CPC Leaky Bucket model and its impact on the timing of snowmelt (Tolwinski-Ward et al., 2011a). Nevertheless, we found clear associations between the four growth parameters. For instance,  $T_1$  and  $T_2$  values and  $M_1$  and  $M_2$  values are clearly associated ( $r = 0.60$  and  $r = 0.47$ , both  $p < 0.01$ ). The often negative correlation between temperature and precipitation at inter-annual time scales is expressed by the inversely related temperature and moisture growth parameters, with the relationship between  $T_2$  and  $M_2$  ( $r = -0.63$ ,  $p < 0.01$ ) being the most noteworthy. Moreover, temperature-limited sites tend to have higher  $T_1$  and  $T_2$  values in comparison to the moisture-limited sites, whereas higher  $M_1$  and  $M_2$  values are characteristic for moisture-limited sites (please refer to Sect. 3.4.1 for the definition of temperature- and moisture-limited sites). This may be an expression of different climatic conditions, but may also be related to edaphic conditions and plant physiological differences.

### 3.3 Relationships between actual and simulated tree-ring growth

The VSL model was able to simulate tree-ring series in response to climate forcing in 2271 out of 2287 sites, clearly demonstrating that the VSL model can be applied to many different environments and species. Nine of the 16 sites not able to be simulated were high-latitude/elevation sites in Nepal (3), Siberia (1), and Canada/Alaska (5) for which no growth was simulated because temperatures never reached the threshold temperature  $T_1$  for growth initiation (hence  $g_T = 0$ ). The remained of the sites not able to be simulated were (sub-) tropical sites in Florida (1), Mexico (4), Argentina (1), and Indonesia (1), for which all annual tree-rings were identical because neither temperature nor moisture were limiting growth (hence  $g_T = 1$  and  $g_M = 1$ ).

The degree of similarity between the 2271 actual  $TRW_{ITRDB}$  and the corresponding modelled  $TRW_{VSL}$  chronologies were determined by Pearson correlation coefficients during the period 1901–1970 (Fig. 1). The average of the Pearson correlation coefficients between all  $TRW_{ITRDB}$  and  $TRW_{VSL}$  is 0.29 and the standard deviation of the correlation coefficients is 0.22. Approximately 41% of the correlation coefficients between  $TRW_{VSL}$  and  $TRW_{ITRDB}$  are statistically significant at the 95% confidence level ( $r > 0.35$ ), taking into account the reduction of degrees of freedom due to autocorrelation (Mitchell et al., 1966). Note, however, that the period 1901–1970 includes the calibration period. Moreover, significant relationships are globally fairly well distributed, with clusters of correlations  $> 0.6$  in the United States. Calibration/verification analysis was performed for two different intervals (1901–1935/1936–1970 and 1936–1970/1901–1935, respectively) and correlation coefficients between  $TRW_{ITRDB}$  and  $TRW_{VSL}$  at each site are taken as measure of model skill. We find significant ( $r > \sim 0.44$ ) correlations during all four calibration/verification intervals for 13.3% of all the series. Further, significant relationships, simultaneously for all of the four calibration/verification periods, can be found on all continents but Africa which generally shows the weakest model stability. Chronologies with highest correlations ( $r > 0.8$ ) for

CPD

9, 4065–4098, 2013

Forward modelling  
of tree-ring width

P. Breitenmoser et al.

Title Page

Abstract

Introduction

Conclusions

References

Tables

Figures

◀

▶

◀

▶

Back

Close

Full Screen / Esc

Printer-friendly Version

Interactive Discussion



all four statistical measures are located in California with further clusters of chronologies in North America where  $r > 0.6$ .

Figure 4 illustrates the year-to-year variability and the mean over all simulated years (1911–1970) of the monthly growth response values  $g_T$  and  $g_M$  for one high-altitude (Fig. 4a) and one low-altitude site (Fig. 4b) in Switzerland. Simulations ( $TRW_{VSL}$ ) as well as the observed chronologies ( $TRW_{ITRDB}$ ) for both sites are shown in Fig. 4c. Because the simulated growth response is controlled by the point-wise minimum of either temperature or moisture, Fig. 4a clearly shows that growth at the high-altitude site is temperature-limited ( $g_T < g_M$ ). The lower elevation site (Fig. 4b), on the other hand, is temperature-limited only briefly at the beginning and at the end of the growing season while moisture limits growth during the summer months ( $g_M < g_T$ ). Additionally, the high-elevation site is negatively correlated with growth at the lower-elevation site, for both the observed and modelled chronologies (with coefficients of  $-0.13$  and  $-0.44$ , respectively). This relationship demonstrates the VSL model's ability to evaluate the joint influence of temperature and moisture on growth. Our simulated growth responses for sites in Switzerland are confirmed by findings from other mountainous regions such as in the southwestern USA (Salzer and Kipfmüller, 2005; Tolwinski-Ward et al., 2011a). Further, the potential of the VSL model to simulate changes over time at a site can be used in the context of future global climate change studies exploring tree-ring growth variability under changing climatic conditions at a particular location.

One-year lagged autocorrelation coefficients (AR1) were assessed from  $TRW_{ITRDB}$  and  $TRW_{VSL}$  series at all sites. Mean coefficients of 0.46 and 0.42, respectively over all series clearly reveal persistence, i.e., 21 % and 18 %, respectively, of the variance in the width of the ring in the current year can be explained by the conditions influencing tree-ring growth in the past year. This highlights the importance of including last year's growing season for growth simulation in the VSL model in order to retain potentially useful climate information contained in tree-rings (see Table 1). Similarly, Wettstein et al. (2011) report median first order autocorrelation coefficients of 0.47 for 762 ITRDB derived tree-ring width series located poleward of roughly 30° to 40° northern latitude

Forward modelling  
of tree-ring width

P. Breitenmoser et al.

Title Page

Abstract

Introduction

Conclusions

References

Tables

Figures

◀

▶

◀

▶

Back

Close

Full Screen / Esc

Printer-friendly Version

Interactive Discussion



## Forward modelling of tree-ring width

P. Breitenmoser et al.

Title Page

Abstract

Introduction

Conclusions

References

Tables

Figures

◀

▶

◀

▶

Back

Close

Full Screen / Esc

Printer-friendly Version

Interactive Discussion



while Tingley et al. (2012) found first order autocorrelation coefficients of approximately 0.6 for the tree-ring width series used in Mann et al. (2008). This reasonable agreement between the autocorrelation structure in modelled versus simulated tree-ring data suggests that mechanistic modelling may be an alternative method capable of mitigating biases in the spectral characteristics of tree-ring chronologies and subsequent climate reconstructions (Meko, 1981; Cook et al., 1999; Franke et al., 2013).

### 3.4 Series aggregation and regional comparison of regional growth variations

#### 3.4.1 Statistically increasing the signal to noise ratio

In the previous sections, the tree-ring chronologies were compared individually with the corresponding CRU grid cell with the underlying assumption that proximity is the best estimate for the climate conditions at a particular site (note the  $0.5^\circ$  or  $\sim 55$  km spatial resolution of the CRU data set at the equator). These analyses allowed exploration of the direct climate–tree ring growth relationship using the VSL model in over 2000 cases. We further demonstrated that the joint influences of temperature and precipitation on tree-ring growth is implemented within the VSL model, and hence, no separation of the climatic influences on growth is needed. Non-climatic noise contained in individual tree-ring chronologies, however, can hinder the detection of clear climate–growth relationships. Hence, we now aggregated tree-ring chronologies to reduce non-climatic noise and to extract regional growth signals. Note, that this statistical-based aggregation method differs from the more typical VSL modelling approach in that (i) the series need to be separated into temperature and moisture limited chronologies and (ii) changes in the limitations over time at a particular site cannot be accounted for in the statistical aggregation approach.

Aggregation is performed using a search radius,  $R$ , alternately of 200 km and 600 km, centred at each land grid cell of the CRU climate data set. The former radius approximates the grid resolution of many global climate models and the latter reflects the large scale at spatially coherent precipitation and especially temperature patterns.

---

**Forward modelling  
of tree-ring width**

P. Breitenmoser et al.

---

Title Page

Abstract

Introduction

Conclusions

References

Tables

Figures

◀

▶

◀

▶

Back

Close

Full Screen / Esc

Printer-friendly Version

Interactive Discussion



The aggregation using a 200 km search radius includes 28 % of all land grid cells and increases to 50 % with a 600 km search radius. The maximum number of individual tree-ring chronologies used for aggregation at 200 and 600 km radii is 111 and 316, while the average number of tree chronologies aggregated at a grid node is 7 and 31, respectively. We do not use greatly expanded search radii like Cook et al. (2010) or Ljungqvist et al. (2012), for instance, whose work were motivated by the construction of a gridded climate reconstruction from spatially sparsely distributed proxy series under considerations of long-range teleconnections (Jones et al., 1997).

We differentiated the sites based upon their principal climatic drivers on growth and thus aggregated separately all temperature and moisture-limited chronologies located within the search radius around each grid cell node. This is particularly important in mountainous terrain with more complex climatic conditions and rapidly changing conditions within small spatial scales influencing tree-ring growth differently (Salzer and Kipfmüller, 2005; see also Fig. 4). Specifically, we classified temperature and moisture sensitive chronologies using the long-term averaged monthly growth responses  $g_T$  and  $g_M$  from the VSL model. Temperature-sensitive chronologies have more temperature- than moisture limited months (i.e., a greater number of months where  $g_T < g_M$ ). All other series are moisture limited (equal or more months with  $g_T > g_M$ ). Aggregated tree-ring width (ATRW) series for temperature and moisture limited series were computed for every grid cell with one or more temperature and/or moisture-limited tree-ring chronologies located within the given search radius. For the 200 (600) km search radii, 10 % (7 %) of all land grid cells contain only temperature-limited series, 7 % (5 %) are only moisture-limited, and 11 % (37 %) of the cells include both temperature- and moisture-limited chronologies.

ATRW from the ITRDB chronologies were defined as weighted mean of the corresponding  $TRW_{ITRDB}$  series found within a specified search circle around each grid node (Eqs. 6–9). Weights were assigned according to four factors: (a) mean  $R_{bar}$  of each chronology, (b) mean EPS of each chronology, (c) distances  $d$  between the site location and the grid node, and (d) the smaller  $\rho$  value of two correlations

## Forward modelling of tree-ring width

P. Breitenmoser et al.

Title Page

Abstract

Introduction

Conclusions

References

Tables

Figures

◀

▶

◀

▶

Back

Close

Full Screen / Esc

Printer-friendly Version

Interactive Discussion



between CRUTS3.1 temperature or precipitation and  $TRW_{ITRDB}$ : for 12 month averages (January–December in the NH, July–June in the SH, respectively) and for 5 month averages for growing season interval (May–September and November–March, respectively). Doing so, we account for persistence while we capture the summer months when climate generally dominates tree growth (Briffa et al., 2002a) and also account for variable growing season lengths at different locations.

Weights are determined by the following functions (see Fig. S1), which vary between 0 and 1:

$$w_{Rbar} = e^{-2(1-Rbar)^5} \quad (6)$$

$$w_{EPS} = e^{-2(1-EPS)} \quad (7)$$

$$w_d = e^{-\frac{2d^2}{R^2}} \quad (8)$$

$$w_p = e^{-3p} \quad (9)$$

There is no a priori reason to choose any particular weighing function but we determined the functions based on theoretical considerations (e.g., Ljungqvist et al., 2012) and the parameter distribution as shown in Table 1. The Gaussian distance weight function was used successfully in Ljungqvist et al. (2012). Multiplication of the four relative weights gives the weight value we apply to each individual tree-ring series within the search radius.

### 3.4.2 VSL simulations for aggregated TRW series

For calculating  $ATRW_{VSL}$  we re-calibrated the VSL simulations for each of the grid cells containing at least one aggregated tree-ring series, using monthly temperature and precipitation series from CRU of that grid cell and with the same VSL model parameter set up described in Table 1. The mean correlation coefficients between  $ATRW_{VSL}$  and  $ATRW_{ITRDB}$  are higher than between  $TRW_{VSL}$  and  $TRW_{ITRDB}$  (which is 0.29). For instance, the average of all coefficients for  $R = 200$  km during the common interval

1901–1970 is 0.34 for the temperature-limited series and 0.38 for the moisture-limited series.

Figure 5 shows the spatial patterns of the correlation coefficients for temperature and moisture-limited ATRW for both search radii. The 600 km search radius improves the relationships for both temperature and precipitation where there was coverage at 200 km but also extends the geographical range which results in lower correlation coefficients. We therefore additionally introduced the condition that at least one chronology must be within 200 km of a grid cell such that both search radii result in the same spatial coverage. Coherent regional scale correlation patterns for temperature limited series can be found in Scandinavia, western/central Siberia, and along western and eastern United States (Fig. 5a and c). Regional correlation patterns for moisture-sensitive series encompass the United States and central Canada (Fig. 5b and d). Regions such as central Europe, Turkey, central Asia, or the Andes are characterised by both temperature and moisture limitations, which is an expression of a complex terrain with small-scale climatic features and large climatic gradients. High correlation coefficients between  $ATRW_{VSL}$  and  $ATRW_{ITRDB}$  are present in all those regions, with a clear tendency towards temperature-limited, high-elevation sites. The broad scale pattern of temperature limited growth for high latitudes (e.g., Taymir peninsula, Russia), and high altitudes (e.g., the European Alps) is in agreement with previous studies (e.g., Briffa et al., 2002a; Wettstein et al., 2011; Babst et al., 2013). Our findings furthermore largely match the distribution of potential climatic constraints to plant growth in Nemani et al. (2003) and Beer et al. (2010) or the climate classification based on Köppen-Geiger by Kottek et al. (2006). Hence,  $ATRW_{VSL}$  and  $ATRW_{ITRDB}$  show spatial coherency and capture the main climate signals and are thus suitable for data assimilation approaches.

In order to employ tree-ring data for climate reconstruction in a data assimilation approach, it is necessary to test if the growth and climate coefficients/relationships apply prior to the calibration period. Accordingly, Fig. 6 shows a scatter plot of the correlation coefficients between the  $ATRW_{VSL}$  and  $ATRW_{ITRDB}$ , 200 km search radius,

CPD

9, 4065–4098, 2013

## Forward modelling of tree-ring width

P. Breitenmoser et al.

Title Page

Abstract

Introduction

Conclusions

References

Tables

Figures

◀

▶

◀

▶

Back

Close

Full Screen / Esc

Printer-friendly Version

Interactive Discussion



during different calibration/verification intervals (1901–1935/1936–1970, and 1936–1970/1901–1935). Points along the 1 : 1 line are sites for which VSL produces simulations that are stable in time whereas points below this line represent sites for which the model yields a higher correlation during the calibration period. We find model skill ( $r > 0.44$ ) in the Pearson correlation coefficients in 36 % of the series during the calibration period, of which 54 % are also significant in the verification period. The model skill is stable for moisture-limited sites in large areas of the United States and central Canada, the lower elevation-sites in west-central Europe, Turkey, Mongolia, western Himalayas, and in mid-Chile whereas temperature-limited sites dominate Scandinavia, Siberia, eastern Himalayas, central Europe, southern-south America, and parts of the western United States. The stability of the VSL model outside the calibration window and its ability to skilfully simulate growth for a wide range of environments promote to use of the model for data assimilation based climate reconstructions, but care must be taken in the selection and aggregation of sites to ensure high signal quality.

## 4 Conclusions

We investigated relationships between climate and tree-ring data on a global scale using the non-linear, process-based Vaganov–Shashkin–Lite (VSL) forward model of tree-ring width formation (Tolwinski-Ward et al., 2011a). A network of 2287 globally distributed ring-width chronologies provided a large, high-quality sample space from which relations among actual tree-ring growth and growth simulated due to climatic influences could be analysed. Bayesian estimation of the VSL growth response parameters performed well for a wide range of species, environmental conditions, and time intervals, showing the model’s general applicability for worldwide studies using CRU climate input data. A benefit from this parameterization approach was also a new global assessment of the growth-onset threshold temperature of approximately 4–6 °C for most sites and species, thus providing new evidence for on-going debates regarding the lower temperatures at which growth may take place (Anchukaitis et al., 2012;

## Forward modelling of tree-ring width

P. Breitenmoser et al.

Title Page

Abstract

Introduction

Conclusions

References

Tables

Figures

◀

▶

◀

▶

Back

Close

Full Screen / Esc

Printer-friendly Version

Interactive Discussion



---

**Forward modelling  
of tree-ring width**P. Breitenmoser et al.

---

[Title Page](#)[Abstract](#)[Introduction](#)[Conclusions](#)[References](#)[Tables](#)[Figures](#)[I ◀](#)[▶ I](#)[◀](#)[▶](#)[Back](#)[Close](#)[Full Screen / Esc](#)[Printer-friendly Version](#)[Interactive Discussion](#)

Mann et al., 2012; Körner, 2012). Moreover, our results demonstrate the VSL model skill to simulate in response to climate variation across a wide range of environments, species, and different time intervals. Further, the model performed well at sites with extreme climate (i.e., classical dendroclimatological sites at treelines) but, in addition, could also reveal notable skill at locations with a less extreme climate due to the models explicit consideration of joint temperature and moisture controls on modelled tree growth. Spatial aggregation of tree-ring chronologies based upon chronology quality, climate response, and proximity reduced non-climatic noise contained in the tree-ring data and resulted in improved relationship between actual and modelled tree-growth as well as a spatial extension of regions where simulations can be validated. The resulting distinct and coherent spatial variability of significant relationships between VSL simulated tree growth and actual tree growth aggregated at 200 km and 600 km further demonstrate the potential of the VSL model to successfully capture the climate signal. This can be exploited, for instance, by using in data assimilation approaches to reconstruct the climate of the past.

**Supplementary material related to this article is available online at:**  
**<http://www.clim-past-discuss.net/9/4065/2013/cpd-9-4065-2013-supplement.pdf>.**

*Acknowledgements.* This work was funded by the Swiss National Science Foundation through the NCCR Climate (projects PALAVAREXIII and DETREE) and Sinergia project FUPSOL. We thank Susan Tolwinski-Ward for providing the MATLAB codes for the VSL model. We also greatly thank the numerous researchers involved in sharing their tree-ring measurements through the International Tree Ring Database (ITRDB) maintained by the NOAA Paleoclimatology Program and the World Data Center for Paleoclimatology and Bruce Bauer for supporting our queries.

## References

- 5 Anchukaitis, K. J., Evans, M. N., Kaplan, A., Vaganov, E. A., Hughes, M. K., Grissino-Mayer, H. D., and Cane, M. A.: Forward modeling of regional scale tree-ring patterns in the southeastern United States and the recent influence of summer drought, *Geophys. Res. Lett.*, 33, L04705, doi:10.1029/2005GL025050, 2006.
- 10 Anchukaitis, K. J., Breitenmoser, P., Briffa, K. R., Buchwal, A., Büntgen, U., Cook, E. R., D'Arrigo, R. D., Esper, J., Evans, M. N., Frank, D., Grudts, H., Gunnarson, B., Hughes, M. K., Kirilyanov, A. V., Körner, C., Krusic, P. J., Luckman, B., Melvin, T. M., Salzer, M., W., Shashkin, A. V., Timmer, C., Vaganov, E. A., and Wilson, R. J. S.: Tree rings and volcanic cooling, *Nat. Geosci.*, 5, 836–837, doi:10.1038/ngeo1645, 2012.
- 15 Babst, F., Poulter, B., Trouet, V., Tan, K., Neuwirth, B., Wilson, R., Carrer, M., Grabner, M., Tegel, W., Levanic, T., Panayotov, M., Urbinati, C., Bouriaud, O., Ciais, P., and Frank, D.: Site- and species-specific responses of forest growth to climate across the European continent, *Global Ecol. Biogeogr.*, 22, 706–717, 2013.
- 20 Beer, C., Reichstein, M., Tomelleri, E., Ciais, P., Jung, M., Bonan, G. B., Bondeau, A., Cescatti, A., Lasslop, G., Lindroth, A., Lomas, M., Luysaert, S., Margolis, H., Oleson, K. W., Rouspard, O., Veenendaal, E., Viovy, N., Williams, C., Woodward, F. I., and Papale, D.: Terrestrial gross carbon dioxide uptake: global distribution and covariation with climate, *Science*, 329, 834–838, 2010.
- 25 Bhend, J., Franke, J., Folini, D., Wild, M., and Brönnimann, S.: An ensemble-based approach to climate reconstructions, *Clim. Past*, 8, 963–976, doi:10.5194/cp-8-963-2012, 2012.
- 30 Briffa, K. R., Osborn, T. J., Schweingruber, F. H., Jones, P. D., Shiyatov, S. G., and Vaganov, E. A.: Tree-ring width and density data around the Northern Hemisphere: Part 1, local and regional climate signals, *Holocene*, 12, 737–757, 2002a.
- Briffa, K. R., Osborn, T. J., Schweingruber, F. H., Jones, P. D., Shiyatov, S. G., and Vaganov, E. A.: Tree-ring width and density data around the Northern Hemisphere: Part 2, spatio-temporal variability and associated climate patterns, *Holocene*, 12, 759–789, 2002b.
- Cook, E. R.: A time series approach to tree-ring standardization, Ph. D. thesis, University of Arizona, 1985.
- Cook, E. R., Briffa, K. R., Shiyatov, S., Mazepa, V., and Jones, P. D.: Data analysis, in: *Methods of Dendrochronology: Applications in the Environmental Sciences*, edited by: Cook, E. R. and Kairiukstis, L. A., Kluwer Academic Publishers, Dordrecht, 1990.

## Forward modelling of tree-ring width

P. Breitenmoser et al.

Title Page

Abstract

Introduction

Conclusions

References

Tables

Figures

◀

▶

◀

▶

Back

Close

Full Screen / Esc

Printer-friendly Version

Interactive Discussion



## Forward modelling of tree-ring width

P. Breitenmoser et al.

[Title Page](#)

[Abstract](#)

[Introduction](#)

[Conclusions](#)

[References](#)

[Tables](#)

[Figures](#)

[◀](#)

[▶](#)

[◀](#)

[▶](#)

[Back](#)

[Close](#)

[Full Screen / Esc](#)

[Printer-friendly Version](#)

[Interactive Discussion](#)



Cook, E. R., Briffa, K. R., Meko, D. M., Graybill, D. A., and Funkhouser, F.: The “segment length curse” in long tree-ring chronology development for palaeoclimatic studies, *Holocene*, 5, 229–237, 1995.

Cook, E. R., Meko, D. M., Stahle, D. W., and Cleaveland, M. K.: Drought reconstructions for the continental United States, *J. Climate*, 12, 1145–1162, 1999.

Cook, E. R., Anchukaitis, K. J., Buckley, B. M., D’Arrigo, R. D., Jacoby, G. C., and Wright, W. E.: Asian monsoon failure and megadrought during the last millennium, *Science*, 328, 486–489, 2010.

Evans, M. N., Reichert, B. K., Kaplan, A., Anchukaitis, K. J., Vaganov, E. A., Hughes, M. K., and Cane, M. A.: A forward modeling approach to paleoclimatic interpretation of tree-ring data, *J. Geophys. Res.*, 111, G03008, doi:10.1029/2006JG000166, 2006.

Fan, Y. and van den Dool, H.: Climate prediction center global monthly soil moisture data set at 0.5° resolution for 1948 to present, *J. Geophys. Res.*, 109, D10102, doi:10.1029/2003JD004345, 2004.

Frank, D., Esper, J., and Cook, E. R.: Adjustment for proxy number and coherence in a large-scale temperature reconstruction, *Geophys. Res. Lett.*, 34, L16709, doi:10.1029/2007GL030571, 2007.

Franke, J., Gonzáles-Rouco, J. F., Frank, D., and Graham, N. E.: 200 yr of European temperature variability: insights from and tests of the Proxy Surrogate Reconstruction Analog Method, *Clim. Dynam.*, 37, 133–150, 2011.

Franke, J., Frank, D., Raible, C., Esper, J., and Brönnimann, S.: Spectral biases in tree-ring climate proxies, *Nat. Clim. Chang.*, 3, 360–364, 2013.

Fritts, H. C.: *Tree Rings and Climate*, Academic Press, London, 1976.

Goosse, H., Crespin, E., de Montety, A., Mann, M. E., Renssen, H., and Timmermann, A.: Reconstructing surface temperature changes over the past 600 yr using climate model simulations with data assimilation, *J. Geophys. Res.*, 115, D09108, doi:10.1029/2009JD012737, 2010.

Grissino-Mayer, H. D. and Fritts, H. C.: The International Tree-Ring Data Bank: an enhanced global database serving the global scientific community, *Holocene*, 7, 235–238, 1997.

Huang, J., van den Dool, H. M., and Georgankakos, K. P.: Analysis of model-calculated soil moisture over the United States (1931–1993) and applications to long-range temperature forecasts, *J. Climate*, 9, 1350–1362, 1996.

## Forward modelling of tree-ring width

P. Breitenmoser et al.

[Title Page](#)

[Abstract](#)

[Introduction](#)

[Conclusions](#)

[References](#)

[Tables](#)

[Figures](#)

[◀](#)

[▶](#)

[◀](#)

[▶](#)

[Back](#)

[Close](#)

[Full Screen / Esc](#)

[Printer-friendly Version](#)

[Interactive Discussion](#)



- Hughes, M. K.: Dendrochronology in climatology: the state of the art, *Dendrochronologia*, 20, 95–116, 2002.
- Hughes, M. K. and Ammann, C. M.: The future of the past – an earth system framework for high resolution paleoclimatology: editorial essay, *Climatic Change*, 94, 247–259, 2009.
- 5 IPCC: Climate Change 2007 The physical science basis, Contribution of working group I to the Forth Assessment Report of the Intergovernmental Panel on Climate Change, edited by: Solomon, S., Qin, D., Manning, M., Chen, Z., Marquis, M., Averyt, K. B., Tignor, M., and Miller, H. L., Cambridge University Press, Cambridge, UK and New York, NY, USA, 2007.
- Jones, P. D., Osborn, T. J., and Briffa, K. R.: Estimating sampling errors in large-scale temperature averages, *J. Climate*, 10, 2548–2568, 1997.
- 10 Jones, P. D., Briffa, K. R., Osborn, T. J., Lough, J. M., van Ommen, T. D., Vinther, B. M., Luterbacher, J., Wahl, E. R., Zwiers, F. W., Mann, M. E., Schmidt, G. A., Ammann, C. M., Buckley, B. M., Cobb, K. M., Esper, J., Goosse, H., Graham, N., Jansen, E., Kiefer, T., Kull, C., Küttel, M., Mosley-Thompson, E., Overpeck, J. T., Riedwyl, N., Schulz, M., Tudhope, A. W., Villalba, R., Wanner, H., Wolff, E., and Xoplaki, E.: High-resolution palaeoclimatology of the last millennium: a review of current status and future prospects, *Holocene*, 19, 3–49, 2009.
- Körner, C.: *Alpine Treelines – Functional Ecology of the Global High Elevation Tree Limits*, Springer, Basel, 2012.
- Körner, C. and Paulsen, J.: A world-wide study of high altitude treeline temperatures, *J. Biogeogr.*, 31, 713–732, 2004.
- 20 Kottek, M., Grieser, J., Beck, C., Rudolf, B., and Rubel, F.: World map of the Köppen–Geiger climate classification updated, *Meteorol. Z.*, 15, 259–263, 2006.
- Ljungqvist, F. C., Krusic, P. J., Brattström, G., and Sundqvist, H. S.: Northern Hemisphere temperature patterns in the last 12 centuries, *Clim. Past*, 8, 227–249, doi:10.5194/cp-8-227-2012, 2012.
- 25 Mann, M. E., Zhang, Z., Hughes, M. K., Bradley, R. S., Miller, S. K., Rutherford, S., and Ni, F.: Proxy-based reconstructions of hemispheric and global surface temperature variations over the past two millennia, *P. Natl. Acad. Sci. USA*, 105, 13252–13257, 2008.
- Mann, M. E., Fuentes, J. D., and Rutherford, S.: Underestimation of volcanic cooling in tree-ring based reconstructions of hemispheric temperatures, *Nat. Geosci.*, 5, 202–205, doi:10.1038/ngeo1394, 2012.
- 30

## Forward modelling of tree-ring width

P. Breitenmoser et al.

Title Page

Abstract

Introduction

Conclusions

References

Tables

Figures

◀

▶

◀

▶

Back

Close

Full Screen / Esc

Printer-friendly Version

Interactive Discussion



- Meko, D. M.: Applications of Box–Jenkins methods of time-series analysis to reconstruction of drought from tree rings, Ph.D. thesis, University of Arizona, 1981.
- Mitchell, J. M. Jr., Dzerdzeevskii, B., Flohn, H., Hofmeyr, W. L., Lamb, H. H., Rao, K. N., and Wallen, C. C.: Climatic change, Technical Note 79, World Meteorological Organization, Geneva, 1996.
- Mitchell, T. D. and Jones, P. D.: An improved method of constructing a database of monthly climate observations and associated high-resolution grids, *Int. J. Climatol.*, 25, 693–712, 2005.
- Nemani, R. R., Keeling, C. D., Hashimoto, H., Jolly, W. M., Piper, S. C., Tucker, C. J., Myeni, R. B., and Running, S. W.: Climate-driven increase in global terrestrial net primary production from 1982 to 1999, *Science*, 300, 1560–1563, 2003.
- Osborn, T. J., Briffa, K. R., and Jones, P. D.: Adjusting variance for sample-size in tree-ring chronologies and other regional time series, *Dendrochronologia*, 15, 89–99, 1997.
- Raible, C. C., Casty, C., Luterbacher, J., Pauling, A., Esper, J., Frank, D., Büntgen, U., Roesch, A. C., Tschuck, P., Wild, M., Vidale, P.-L., Schär, C., and Wanner, H.: Climate variability – observations, reconstructions, and model simulations for the Atlantic–European and Alpine region from 1500–2100 AD, *Climatic Change*, 79, 9–29, 2006.
- Rossi, S., Deslauriers, A., Anfodillo, T., and Carraro, V.: Evidence of threshold temperatures for xylogenesis in conifers at high altitudes, *Oecologia*, 152, 1–12, 2007.
- Salzer, M. W. and Kipfmüller, K. F.: Reconstructed temperature and precipitation on a millennial timescale from tree-rings in the southern Colorado Plateau, USA, *Climatic Change*, 70, 465–487, 2005.
- Shi, J., Liu, Y., Vaganov, E. A., Li, J., and Cai, Q.: Statistical and process-based modeling analyses of tree growth response to climate in semi-arid area of north central China: A case study of *Pinus tabulaeformis*, *J. Geophys. Res.*, 113, G01026, doi:10.1029/2007JG000547, 2008.
- Tingley, M. P., Craigmile, P. F., Haran, M., Li, B., Mannshardt, E., and Rajaratnam, B.: Piecing together the past: statistical insights into paleoclimatic reconstructions, *Quaternary Sci. Rev.*, 35, 1–22, 2012.
- Tolwinski-Ward, S. E., Evans, M. N., Hughes, M. K., and Anchukaitis, K. J.: An efficient forward model of the climate controls on interannual variation in tree-ring width, *Clim. Dynam.*, 36, 2419–2439, 2011a.

**Forward modelling  
of tree-ring width**

P. Breitenmoser et al.

[Title Page](#)[Abstract](#)[Introduction](#)[Conclusions](#)[References](#)[Tables](#)[Figures](#)[I◀](#)[▶I](#)[◀](#)[▶](#)[Back](#)[Close](#)[Full Screen / Esc](#)[Printer-friendly Version](#)[Interactive Discussion](#)

- Tolwinski-Ward, S. E., Evans, M. N., Hughes, M. K., and Anchukaitis, K. J.: Erratum to: An efficient forward model of the climate controls on interannual variation in tree-ring width, *Clim. Dynam.*, 36, 2441–2445, 2011b.
- 5 Tolwinski-Ward, S. E., Anchukaitis, K. J., and Evans, M. N.: Bayesian parameter estimation and interpretation for an intermediate model of tree-ring width, *Clim. Past Discuss.*, 9, 615–645, doi:10.5194/cpd-9-615-2013, 2013.
- Touchan, R., Shishov, V. V., Meko, D. M., Nouri, I., and Grachev, A.: Process based model sheds light on climate sensitivity of Mediterranean tree-ring width, *Biogeosciences*, 9, 965–972, doi:10.5194/bg-9-965-2012, 2012.
- 10 Trouet, V., Esper, J., Graham, N. E., Baker, A., and Frank, D.: Persistent positive North Atlantic Oscillation Mode dominated the Medieval Climate Anomaly, *Science*, 324, 78–80, 2009.
- Vaganov, E. A., Hughes, M. K., and Shashkin, A. V.: Growth dynamics of conifer tree rings, in: *Growth Dynamics of Tree Rings: Images of Past and Future Environments*, Ecological studies, 183, Springer, New York, 2006.
- 15 Vaganov, E. A., Anchukaitis, K. J., and Evans, M. N.: How well understood are the processes that create dendroclimatic records?, A mechanistic model of climatic control on conifer tree-ring growth dynamics, in: *Dendroclimatology, Developments in Paleoenvironmental Research*, 11, edited by: Hughes, M. K., Swetnam, T., and Diaz, H., Springer, New York, 2011.
- van den Dool, H., Huang, J., and Fan, Y.: Performance and analysis of the constructed analogue method applied to US soil moisture over 1981–2001, *J. Geophys. Res.*, 108, 8617, doi:10.1029/2002JD003114, 2003.
- Wahl, E. and Frank, D.: Evidence of environmental change from annually-resolved proxies with particular reference to dendroclimatology and the last millennium, in: *The SAGE Handbook of Environmental Change*, 1, edited by: Matthews, J. A., Sage, 320–344, 2012.
- 25 Wallace, J. M. and Hobbs, P. V.: *Atmospheric Science: an Introductory Survey*, 2nd Edn., International Geophysics Series, 92, Elsevier Academic Press, Amsterdam, 2006.
- Wettstein, J. J., Littell, J. S., Wallace, J. M., and Gedalof, Z.: Coherent region-, species-, and frequency-dependent local climate signals in Northern Hemisphere tree-ring widths, *J. Climate*, 24, 5998–6012, 2011.
- 30 Widmann, M., Goosse, H., van der Schrier, G., Schnur, R., and Barkmeijer, J.: Using data assimilation to study extratropical Northern Hemisphere climate over the last millennium, *Clim. Past*, 6, 627–644, doi:10.5194/cp-6-627-2010, 2010.

Wigley, T. M. L., Briffa, K. R., and Jones, P. D.: On the average value of correlated time series, with applications in dendroclimatology and hydrometeorology, *J. Climate Appl. Meteorol.*, 23, 201–213, 1984.

5 Zhang, Y. X., Shao, X. M., Xu, Y., and Wilmking, M.: Process-based modelling analyses of *Sabina przewalskii* growth response to climate factors around the northeastern Qaidam Basin, *Chinese Sci. Bull.*, 56, 1518–1525, 2011.

**Forward modelling  
of tree-ring width**

P. Breitenmoser et al.

Title Page

Abstract

Introduction

Conclusions

References

Tables

Figures

⏪

⏩

◀

▶

Back

Close

Full Screen / Esc

Printer-friendly Version

Interactive Discussion



## Forward modelling of tree-ring width

P. Breitenmoser et al.

**Table 1.** VSL model parameters.

Parameter description	Parameter	Value
Temperature response parameters		
Threshold temp. for $g_T > 0$	$T_1$	$\epsilon$ [1 °C, 9 °C]
Threshold temp. for $g_T = 1$	$T_2$	$\epsilon$ [10 °C, 24 °C]
Moisture response parameters		
Threshold soil moist. for $g_M > 0$	$M_1$	$\epsilon$ [0.01, 0.035] v/v
Threshold soil moist. for $g_M = 1$	$M_2$	$\epsilon$ [0.1, 0.7] v/v
Soil moisture parameters		
Runoff parameter 1	$\alpha$	0.093 month <sup>-1</sup>
Runoff parameter 2	$\mu$	5.8 (dimensionless)
Runoff parameter 3	$m$	4.886 (dimensionless)
Max. moisture held by soil	$W_{\max}$	0.8 v/v
Min. moisture held by soil	$W_{\min}$	0.01 v/v
Root (bucket) depth	$d_r$	1000 mm
Integration window parameters		
Integration start month	$l_0$	-4
Integration end month	$l_f$	12

Title Page

Abstract

Introduction

Conclusions

References

Tables

Figures

◀

▶

◀

▶

Back

Close

Full Screen / Esc

Printer-friendly Version

Interactive Discussion



## Forward modelling of tree-ring width

P. Breitenmoser et al.

**Table 2.** Statistics of the Bayesian estimation of the site-by-site tuned VSL growth response parameters  $T_1$ ,  $T_2$ ,  $M_1$ , and  $M_2$  for the 1901–1935 and 1936–1970 calibration intervals.

	Calib. 1: 1901–1935				Calib. 2: 1936–1970			
	mean	min	max	std	mean	min	max	std
$T_1$ (°C)	4.64	1.80	8.41	0.93	4.75	1.74	7.97	0.89
$T_2$ (°C)	16.34	10.14	22.80	1.62	16.52	10.36	21.87	1.59
$M_1$ (v/v)	0.023	0.02	0.025	0.001	0.023	0.019	0.025	0.001
$M_2$ (v/v)	0.44	0.11	0.64	0.09	0.43	0.11	0.64	0.09

[Title Page](#)
[Abstract](#)
[Introduction](#)
[Conclusions](#)
[References](#)
[Tables](#)
[Figures](#)
[I ◀](#)
[▶ I](#)
[◀](#)
[▶](#)
[Back](#)
[Close](#)
[Full Screen / Esc](#)
[Printer-friendly Version](#)
[Interactive Discussion](#)


Forward modelling  
of tree-ring width

P. Breitenmoser et al.

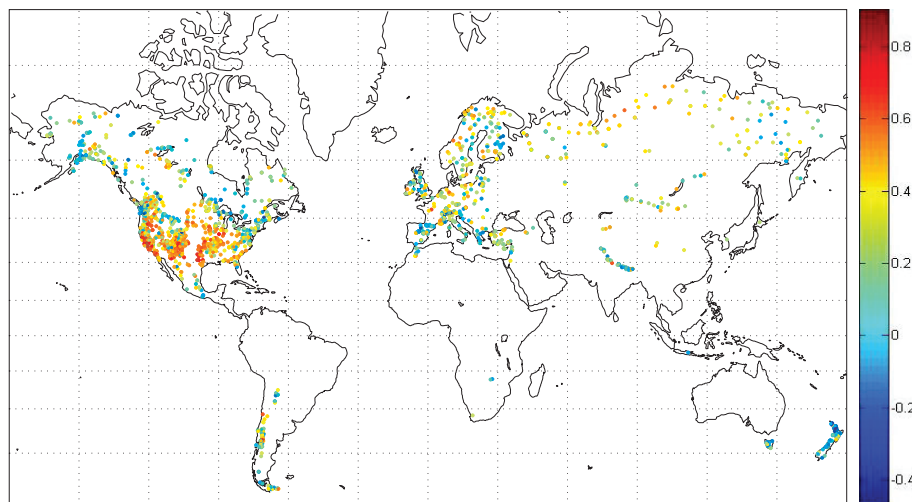


**Fig. 1.** Locations of the 2287 tree-ring width chronologies ( $TRW_{ITRDB}$ ) and the correlation coefficients between  $TRW_{ITRDB}$  and  $TRW_{VSL}$  for 1901–1970.

[Title Page](#)[Abstract](#)[Introduction](#)[Conclusions](#)[References](#)[Tables](#)[Figures](#)[◀](#)[▶](#)[◀](#)[▶](#)[Back](#)[Close](#)[Full Screen / Esc](#)[Printer-friendly Version](#)[Interactive Discussion](#)

## Forward modelling of tree-ring width

P. Breitenmoser et al.

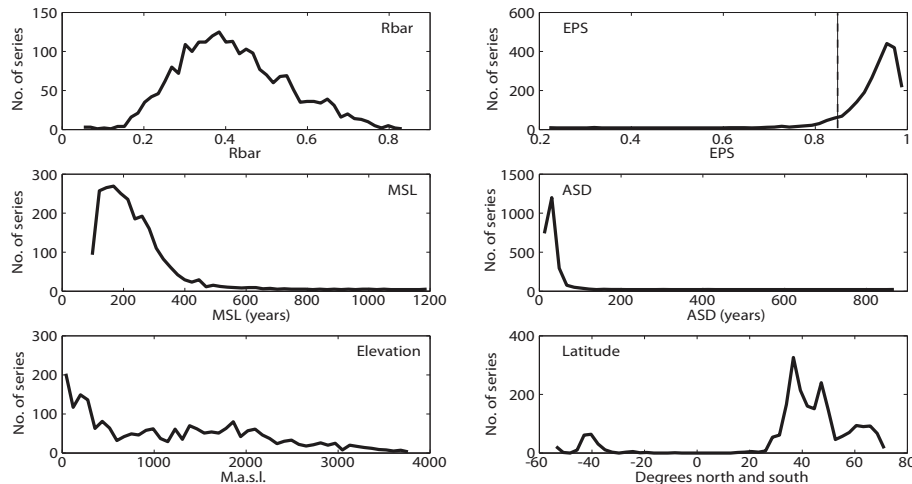


**Fig. 2.** Chronology characteristics for 1901–1970. Rbar is the average inter-series correlation between all series from different trees (Cook et al., 1990); EPS is the expressed population signal and the vertical line denotes the commonly cited 0.85 EPS criterion (Wigley et al., 1984; Cook et al., 1990). Mean 1901–1970 Rbar and EPS values were calculated using a 30 yr window that lags 15 yr; MSL is the mean segment length; and ASD is the average sample depth (48 bins were distinguished in each variable).

Title Page

Abstract

Introduction

Conclusions

References

Tables

Figures

◀

▶

◀

▶

Back

Close

Full Screen / Esc

Printer-friendly Version

Interactive Discussion



## Forward modelling of tree-ring width

P. Breitenmoser et al.

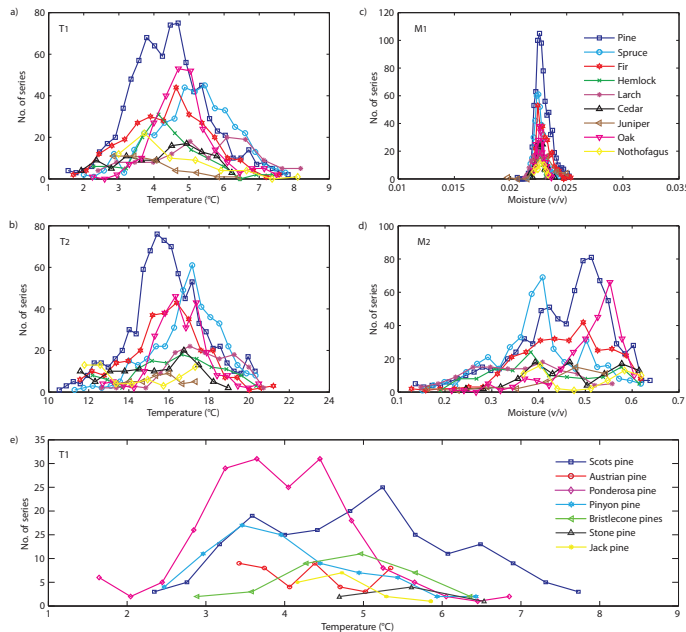


**Fig. 3.** Bayesian estimated VSL growth response parameters: **(a)**  $T_1$ , lowest threshold temperature; **(b)**  $T_2$ , lower bound for optimal temperature; **(c)**  $M_1$ , lowest threshold for moisture; **(d)**  $M_2$ , lower bound for optimal moisture parameters calculated during 1911–1970 for different tree genera: pine (*pinus*;  $n = 821$ ), spruce (*picea*;  $n = 407$ ), fir (*abies*;  $n = 286$ ), hemlock (*tsuga*;  $n = 124$ ), larch (*larix*;  $n = 126$ ), cedar (*cedrus*;  $n = 107$ ), juniper (*juniperus*;  $n = 40$ ), oak (*quercus*;  $n = 253$ ), and southern beech (*nothofagus*;  $n = 62$ ).  $T_1$  threshold temperature for different pine species **(e)**: Scots pine (*Pinus sylvestica*;  $n = 172$ ), Austrian pine (*Pinus nigra*;  $n = 45$ ), Ponderosa pine (*Pinus ponderosa*;  $n = 181$ ), Pinyon pine (*Pinus edulis*;  $n = 73$ ), Bristlecone pine (*Pinus aristata*, *Pinus longaeva*, and *Pinus balfouriana*;  $n = 34$ ), Stone pine (*Pinus pinea*;  $n = 7$ ), and Jack pine (*Pinus banksianac*;  $n = 15$ ). Numbers in brackets give the series contributing in each group of tree genera. The number of bins for each parameter is determined through the square root of its length.

[Title Page](#)
[Abstract](#)
[Introduction](#)
[Conclusions](#)
[References](#)
[Tables](#)
[Figures](#)
[◀](#)
[▶](#)
[◀](#)
[▶](#)
[Back](#)
[Close](#)
[Full Screen / Esc](#)
[Printer-friendly Version](#)
[Interactive Discussion](#)

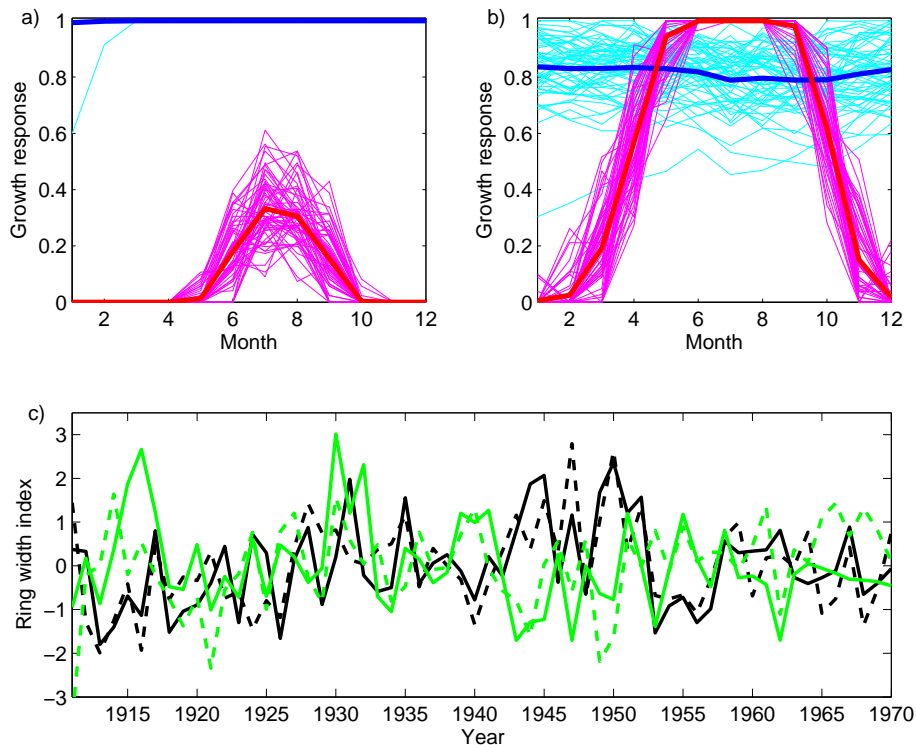



**Fig. 4.** Simulated monthly growth response curves for each year (1911–1970) for temperature ( $g_T$ , magenta lines) and moisture ( $g_M$ , cyan lines) for two sites in Switzerland **(a)** Bergün Val Tuors, European larch, 2065 m, and **(b)** Krauchthal, Scots pine, 550 m. The long-term (1911–1970) mean value is overlaid in red for temperature and in blue for moisture; **(c)** TRW<sub>ITRDB</sub> and TRW<sub>VSL</sub> (dashed lines) for Bergün Val Tuors (black lines),  $r = 0.69$ ,  $p < 0.01$  and Krauchthal (green lines),  $r = 0.44$ ,  $p < 0.01$ .

[Title Page](#)
[Abstract](#)
[Introduction](#)
[Conclusions](#)
[References](#)
[Tables](#)
[Figures](#)
[I ◀](#)
[▶ I](#)
[◀](#)
[▶](#)
[Back](#)
[Close](#)
[Full Screen / Esc](#)
[Printer-friendly Version](#)
[Interactive Discussion](#)


## Forward modelling of tree-ring width

P. Breitenmoser et al.

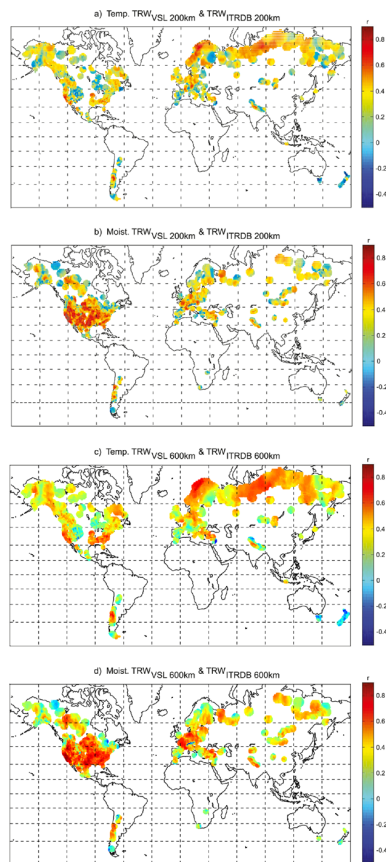


**Fig. 5.** Pearson correlation coefficients between  $ATRW_{VSL}$  and  $ATRW_{ITRDB}$  for a search radius of 200 km (**a**, **b**) and 600 km (**c**, **d**) at temperature-limited (**a**, **c**) and moisture-limited (**b**, **d**) grid cells. Note that in panels (**c**) and (**d**) at least one chronology has to be within the 200 km search radius to make the correlations comparable.

Forward modelling  
of tree-ring width

P. Breitenmoser et al.

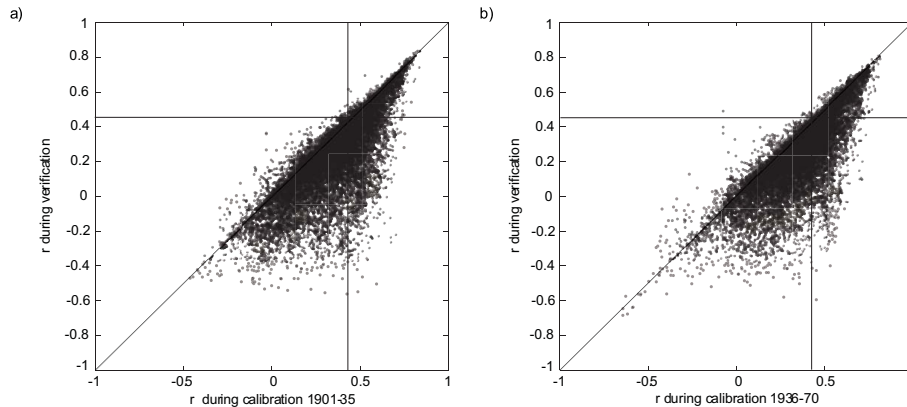


**Fig. 6.** Scatter plot of correlation coefficients between  $ATRW_{VSL}$  and  $ATRW_{ITRDB}$  (200 km search radius) series for two different calibration/verification intervals **(a)** 1901–1935/1936–1970; and **(b)** 1936–1970/1901–1935.

[Title Page](#)[Abstract](#)[Introduction](#)[Conclusions](#)[References](#)[Tables](#)[Figures](#)[◀](#)[▶](#)[◀](#)[▶](#)[Back](#)[Close](#)[Full Screen / Esc](#)[Printer-friendly Version](#)[Interactive Discussion](#)